Modelling of Lintel-Masonry Interaction Using COMSOL

A.T. (Ad) Vermeltfoort & A. W. M. (Jos) van Schijndel
Eindhoven University of Technology
P.O. Box 513; 5600 MB Eindhoven; Netherlands
a.t.vermeltfoort@tue.nl

Abstract: Usually, when using Finite Element Models, structures are subdivided into elements and uniform properties are assigned to each material. However, in masonry, like in many other materials, properties vary over the volume of the structure.
Therefore an attempt was made, as described in this paper, to assign material properties like shear strength and modulus of elasticity randomly. In this way, the behaviour of a masonry wall with a prefabricated concrete lintel was experimentally tested and simulated using COMSOL. The paper confirms the possible use of COMSOL for modelling lintel-masonry interaction, including variation of mechanical properties over the volume of the specimen. It shows the relatively small effect of variation of the E-modulus on the load distribution and the relatively large effect of shear strength on the failure load.

Keywords: Lintels, masonry, shear strength, random properties, experiments, simulation

1. Introduction

To span openings in masonry walls often a concrete beam is used. In this situation the beam is called a lintel. Together with the masonry the lintel carries the load. In experiments, a relatively large variation of the load bearing capacity of this type of structures is found. Experiments are expensive and not all parameters are easy to reproduce. Therefore an attempt was made to simulate this type of testing by assigning random values for modulus of elasticity and strength to each individual brick.

In this paper the modelling of the experimental observed lintel-masonry interaction using COMSOL is presented in combination with the experiments. The main reason to use COMSOL is the relative easy implementation of a more advanced way to model the differences in bricks and joints. This pre-processing technique is shown in Section 4.2. The modelling in COMSOL is quite straight forward. Another development is the post processing of the shear stress concentration near the supports for predicting the maximum load. This development is discussed in Section 5.3 after the presentation of detailed shear experiments.

2. Experimental program and implementation in simulations

Three series of three lintel-wall combinations were experimentally tested to failure. The main parameter in the research project was the support condition, which will be discussed in section 3.2.

2.1. Specimen and test set-up

The test-walls had a span of 2.8 meters; their height was 60 mm for the lintel with nine layers of masonry (562.5 mm) on top. i.e. 622.5 mm total height. Figure 1 shows a photograph and Figure 2 shows schematically the set-up of the four point bending test.

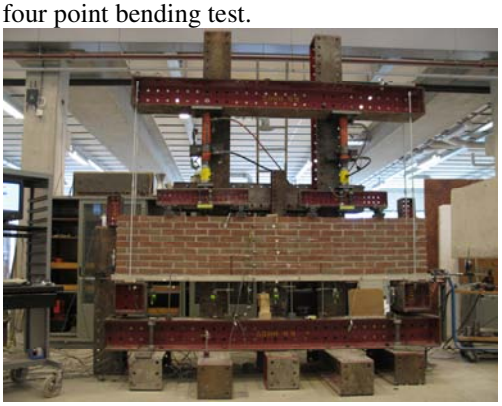

Figure 1. Lintel-wall test set-up

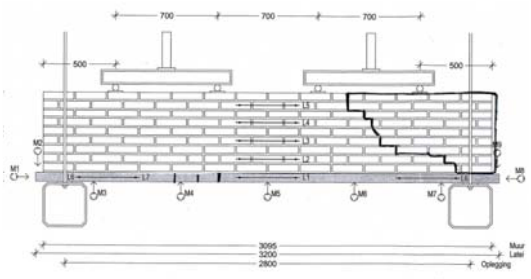

Figure 2. Load introduction scheme and cracked wall

The load is formed by four forces that were applied by means of two jacks and two load distribution beams and simulated a uniform distributed load.
Various deformation measurements were made to observe overall behaviour and to allow for detection of cracks (only briefly mentioned in this paper).

2.2. Implementation in COMSOL

The plane strain application (2D) mode is used. We refer to the COMSOL User's Guide for the theory background. Figure 3 shows the geometry and the different domains. The corresponding sub domain setting properties are discussed later in section 4.2.

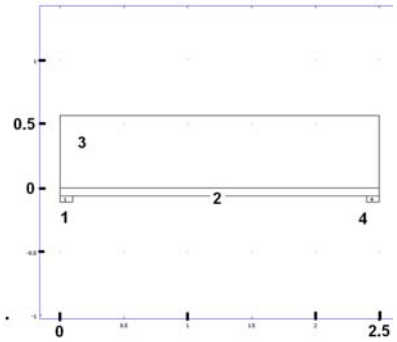

Figure 3. Geometry and domains

2.3. Building of the specimens

The test-walls were all built in the same way and materials of the same quality were used. First, nine walls were build on three different days. Then the support condition was randomly assigned to each test wall. To control and establish the variation of material properties, smaller specimens build together with the test walls, were tested in shear.

3. Types of support

The structure above openings in masonry walls with lintels can be schematized as a 2-D structure. Their thickness, usually equal to the width of a brick (approximately 100 mm) is small compared to the length and height of the structure. Supporting surfaces have a length between 100 and 200 mm. Two extreme situations can be recognized for the support surface: complete freedom of movement in horizontal direction i.e. parallel to the length of the lintel and completely confined i.e. no horizontal movement at all. Vertically, the movement was confined completely. In building practice, the rotation may be partly confined (rotation spring). However, that is no parameter in this research. It was assumed that the lintel rested on its support and that only compression could occur.

3.1. Support conditions in the simulations

The horizontally completely free support condition was modelled. Therefore, boundary properties were assigned to edges and points that represented the support boundaries. The corresponding boundary properties for edges are set to zero (free movement) except for the edges that represented the support surfaces. These edges were confined vertically (no movement at all).

A load of -10^4 N/m^2 was applied to the roof edge of the specimen. The boundary conditions at specific points are set to zero (free movement in horizontal direction) or set to one to confine that specific point to move, that means $\delta x = 0$.
A point at the top edge of the wall and on the vertical line of symmetry is confined to obtain proper equilibrium conditions.

The uniform load applied in the simulations differs from the four point loading in the experiments. In the experiments the distances between the four loads of equal magnitude – $P = 0.25ql$ – was 0.25 times the length of the wall. In this way, the maximum shear forces in the beam and the maximum bending moment are equal for both the uniform distributed and the four point loading. See e.g. Meriam and Kraige (2008). The maximum shear force is $V = 0.5ql$, the maximum bending moment equals $M = 0.125ql^2$. The load and shear distribution are schematically shown in Figure 4.

3.2. Support conditions in the experiments

Figure 5 shows details of the three types of support used in the tests.
a. Two steel blocks were suspended from the roof beam of the test frame each with two

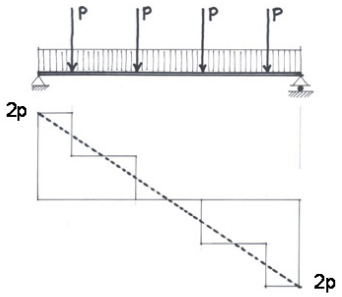

Figure 4. Shear force distribution along the length of the wall for a uniform load and a four point loading.

threaded steel bars, 1.50 m long, and 16 mm in diameter. The test-wall was positioned between the bars on the steel blocks. In this way, the steel block could sway freely in horizontal direction. This is called support type R (Roller).
b. By mounting the same steel blocks on the bottom beam of the test frame a hinged support was made which means no vertical nor horizontal movement, however, free to rotate. This is called support type H (Hinge)
c. In a brick wall, a lintel may be confined lengthwise. In the most extreme situation the lintel can not elongate. To simulate this in the tests, steel plates were used at the end of the lintel. The steel plates were connected to each other by four threaded bars that ran parallel to the lintel. This additional structure in combination with the lintel formed a stiff tensor. This is called support type S (Stiffened tensor).

In building practice, a lintel rests on a piece of masonry and some kind of material (e.g. a 5 mm thick rubber sheet) is used to allow for dimensional tolerances and a smooth load transfer from lintel to brickwork. This situation was simulated in the tests by a piece of soft board.

4. Material properties

4.1. Masonry properties

All test walls and shear specimens were made using Rijswaard soft mud brick in combination with an industrially composed mortar. The mortar was prepared and applied in a similar manor for all test-walls and small specimens. All variation in the mortar properties was unintended and due to practical effects. Per mortar batch, six mortar prisms were prepared and tested according PrEN 1052-3:2001. This gave an averaged compressive mortar strength of 9.60 N/mm^2 with a coefficient of variance (C.o.V.) of 18.5 % in 54 tests.

The Rijswaard soft mud clay bricks had a compressive strength of 27 N/mm^2 and a C.o.V. of 12 %.

These properties are meant to characterize the materials. However, to have properties for numerical simulations, small masonry specimens, more similar to the masonry in the test walls have to be prepared and tested like the specimens used for shear tests.
From other research it is known that the modulus of elasticity for the type of masonry used varies between 3500 N/mm^2 and 8000 N/mm^2, Vermeltfoort et al. (2007).

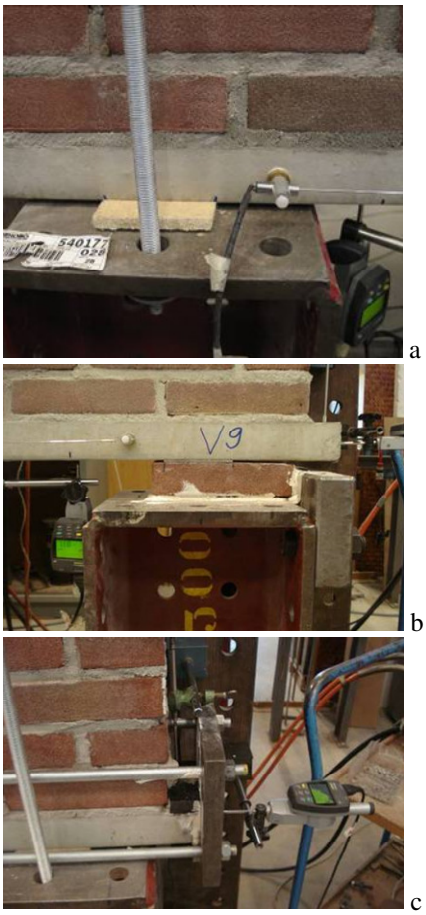

a
b
c

Figure 5. Types of support, a) steel block and soft board, b) brick with soft board and c) stiffened tensor.

4.2. Modelling different bricks

The basic idea is to model the masonry wall as a continuous distribution of the Young's modulus (E). The goal is to find E = Efun(x,y) for a fine grid for the whole wall including the stochastic nature of each brick. The methodology consisted on three steps: First, the use of a method to assign values (uniform random numbers between 2 10^9 and 6 10^9 Pa) for the Young's modulus for each brick. Second, the creation a fine grid using nearest neighbour interpolation so that inside each brick the Young's modulus is constant. Third, the export of the fine grid results (2D) to a COMSOL function. MatLab was used to implement the steps. Figure 7 shows the code used and the results are shown in figure 6 where the variation in colours indicates the variation in Young's modulus in the brick wall. The corresponding sub domain setting properties are (see also section 2.2) given in Table 1.

Table 1 Sub domain setting properties

Sub domain		1, 4	2	3
Young's modulus (E)	Pa	5e9	35e9	Efun(x,y)
Density (rho)	kg/m^3	2500	2500	2000
Poisson's ratio (nu)	1	0.3	0.3	0.2
Sub domain 1 and 4 represent the support blocks , sub domain 2 is the concrete lintel and sub domain 3 represents masonry.				

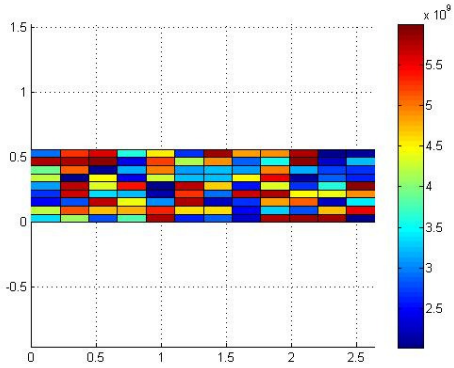

Figure 6. The E distribution of the brick wall. Values range between 2.10^9 N/m^2 and 6.10^9 N/m^2.

```
 Position of the bricks
x=      [0:0.22:12*0.22];
y=      [0:0.0625:9*0.0625];

 Number of bricks
nx=length(x);
ny=length(y);

 mesh
[xx,yy] = meshgrid(x,y);

 Fine grid
x2=0:0.02:12*0.22;
y2=0:(0.0625/4):9*0.0625;
[xi,yi] = meshgrid(x2,y2);

STEP 1: Uniform between 2e9 and 4e9
Exy=2e9+4e9*rand(ny,nx);
%STEP 2: interpolate on fine grid
data=interp2(xx,yy,Exy,xi,yi,'nearest');

STEP 3:Create data structure for COMSOL
Efun.x=x2;
Efun.y=y2;
Efun.data=data;
```

Figure 7. The Matlab code to model different bricks

4.3. Shear experiments

Shear test specimens were build of three bricks and two joints simultaneously with, and in the same manor as the test walls. Over a year, one specimen was made for each 100 bricks that were used to build test walls for this project and various other projects. In total sixty specimens with ideally the same mortar and the same type of soft mud bricks were tested.

Shear strength of these three-brick-two-joint specimens was established according with NEN EN 1052-3. A test-set-up as shown in Figure 8 was used.

The main principle of this masonry shear test is that the central brick is sheared from in-between the two bricks at the outside. This loading situation is similar to the critical situation in the simulated lintel-wall configuration. In each test, the pre-loading, perpendicular to the shear direction, may be different. Three pre-loading levels are prescribed in NEN EN 1052-3.

Two jacks, one horizontal for pre-compression and one vertical for shear loading, were mounted in a steel frame, Figure 8. The supports and the load introduction points allowed for some adjustments as masonry specimens have some dimensional variation and surfaces are not always exactly parallel.

Figure 8 Shear test-set-up with a three-brick-two-joint specimen.

4.4. Shear test results

In Figure 9 the maximum recorded shear strength was plotted versus the applied pre-stress for each test separately. Stresses are established using a gross loaded area of one brick, 96 x 206 mm^2.

The initial data set of sixty results shows low results for a number of specimens. Some of these values were from specimens in which mortar-brick-bond was broken, probably due to shrinkage, Vermeltfoort et al. (2007). Another possible cause for a low result may have been the positioning in the set-up which caused unequal introduction of the pre-load. Neglecting these low values results for the remaining 49 tests in the following equation:

$$\tau_{ini} = 0.66 \cdot \sigma + 0.33 \qquad (1)$$

Another analysis shows that the age of the specimen has no significant effect on shear strength.
For COMSOL simulations a shear strength of 0.25 N/mm^2 with a standard deviation of 0.08 N/mm^2 was used. The application of these results will be discussed in Section 5.3.

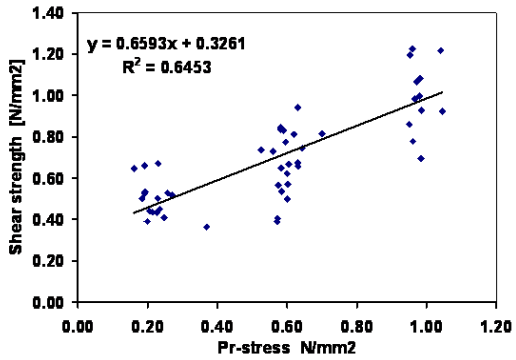

Figure 9 Shear strength versus pre-stress

5. Results

5.1. Experimental results

In Table 1 values for the load at which the first crack appeared and the ultimate load are given. The appearance of cracks was observed during testing and verified after testing by observing load deformation graphs. The load-mid-span-deflection graph for nine tests is plotted in Figure 10. In some cases, cracking and failure coincided, in other cases some load increase was still possible, shown by the values per test in the two columns on the right hand side in Table 1. The results indicate that the support condition has an effect on the load bearing capacity. The results also show variation in results roughly of a factor two between the lowest (73 kN) and the highest (160 kN) cracking load values.

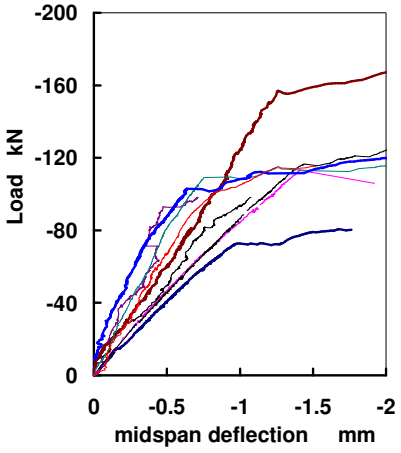

Figure 10 Load deflection graphs for three times three walls.

Figure 11 shows a cracking pattern typical for all tests. The cracking patterns indicate that pieces of masonry shear over the joint between lintel and masonry after the masonry cracked on the bottom at mid span. Therefore, a shear failure criterion was used in the simulations.

Table 1 Test program and main results (total load and load in kN per m^2)

		mortar	load			
test	Su	f's	cracking		ultimate	
no		MPa	*)	**)	*)	**)
1	R	0.29	110	360	125	400
2	R	0.26	112	360	125	400
3	R	0.25	105	340	118	380
4	H	0.32	73	240	81	260
5	H	0.33	117	380	117	380
6	H	0.40	118	380	161	520
7	S	0.31	82	260	98	320
8	S	0.32	85	270	99	320
9	S	0.39	160	520	178	580

*) total load over the full length in kN
**) uniform load per unit area in kN/m^2.
Su.: Support conditions
R: free horizontal movement,
H: confined horizontal movement,
f's: shear strength
S: stiffened tensor

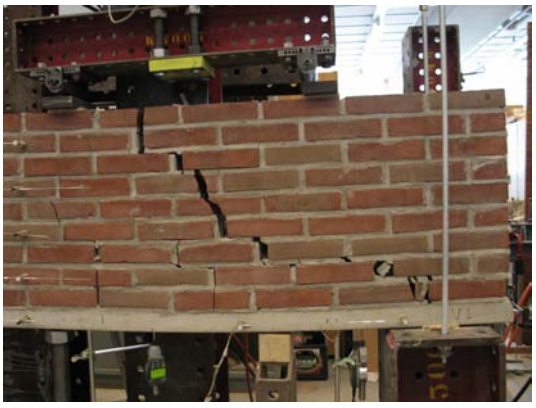

Figure 11 Example of a cracked wall, indicating shear near the support in the joint between lintel and masonry.

5.2. Results of COMSOL simulations

As known from experiments, shear is the dominant failure mode for lintel-masonry assemblies. Therefore, the shear stress (sxy) distribution over the wall was established using the described model and plotted in Figure 12. The shear stress distribution at the lintel-masonry interface (i.e. at y = 0), found with COMSOL simulations is shown in Figure 13. This distribution indicates, as expected, stress concentrations near the supports.

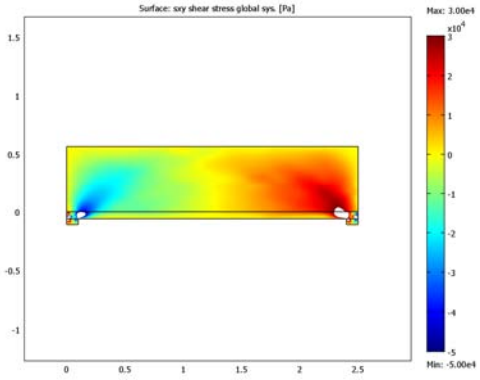

Figure 12. The shear stress distribution over the wall indicates large shear stresses in the interface between lintel and masonry near the supports.

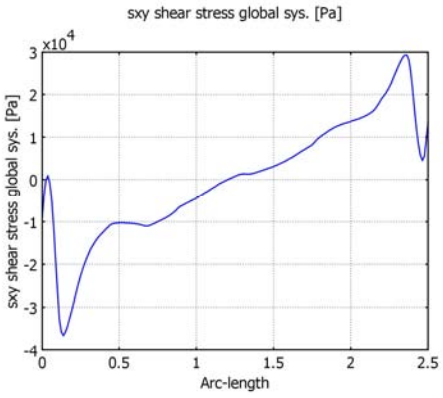

Figure 13. The shear stress profile at y=0

For design purposes, the lintel-wall configuration may be represented as a beam on two supports loaded by a uniform load (q) or four point loads (P = 0.25 ql). Usually, it is sufficient to assume a point support for design calculations, however, in this analyses it is assumed that the support produces a triangular reaction stress block.

In the masonry, a compression arch, following the line of thrust will develop, Wood (1952). This arch produces a higher loading near the supports than in the centre. Due to this arching effect, less load will be transferred via the central part of the lintel. This load transfer mechanism is confirmed by cracks in the bed joint between the lintel and the masonry at mid span.
Based on these observations, a load distribution as shown in Figure 14 is assumed (triangular reaction stresses and increased loading near the support). This load distribution produces a shear force distribution along the length of the beam, as shown in Figure 15.

The shear stress distribution will have the same shape because shear stress is linear related to shear forces. Comparing Figure 13 with Figure 15 shows the resemblance in the shear stress distribution. As the load concentrates on the inside of the supports, due to arch-action, stresses will concentrate near the supports. At mid-span, shear is less affected by reaction effects as also follows from Figure 12.

For comparison with the experiments, the vertical displacements were calculated. Figure 16 shows the deformed specimen and indicates the vertical (Y) displacements for a total load of 100 kN. This load of 100 kN acts on a surface of 0.1m x 2.5m which results in an equally distributed load of 4 10^5 N/m^2.
The deformation for the simulation - in this case of 1.347 mm - differs from the mean experimental value of approximately 0.90 mm.

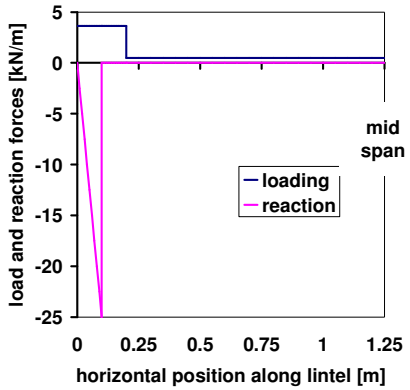

Figure 14. Loading on the left part of the lintel, increased load near the support, triangularly distributed reaction stresses.

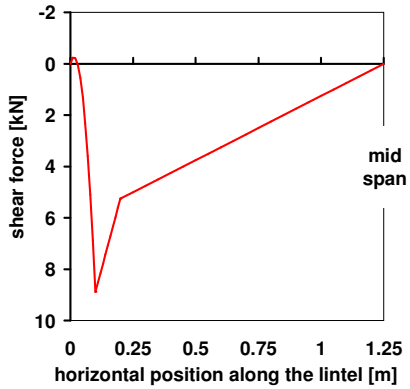

Figure 15 Shear force distribution along length of the lintel (from left to mid span) for the loading situation given in Figure 14.

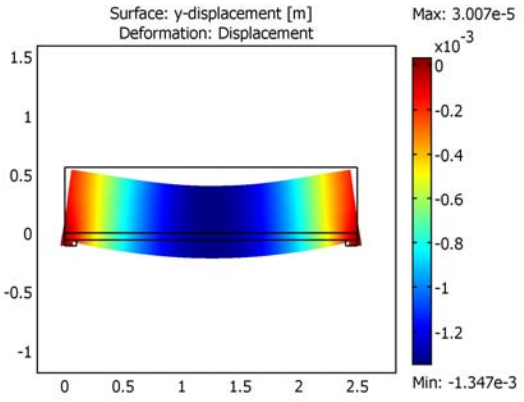

Figure 16. The displacement for a load of 4 10^5N/m^2

5.3. Estimation of the failure load

To estimate the failure load using the simulated data the next three-step methodology was implemented in MatLab.
First, the shear stresses at the interface between concrete lintel and masonry – y = 0 in Figure 3 - were established with simulations for nine walls with identical dimensions but with varying E-values. In Figure 17 the absolute value of the shear stress is plotted versus the length of the lintel. Each line represents one simulation.

Figure 17 shows the effect of the variations in the E distribution on the shear stress. The variation in magnitude (the band width) is relatively small compared to the maximum value. As mentioned earlier, the highest shear stresses near the supports will lead to fracture.

Second, the shear strength of each brick at the y = 0 level (the interface between lintel and masonry) was varied using a normal distribution with a mean value of 0.25 N/mm^2 and a standard deviation of 0.08 N/mm^2.

This process was also repeated nine times.
The third and last step was to multiply each simulated shear stress profile with a factor in such a way that the curve 'just touches' the shear strength curve. As expected, the positions where both lines 'touch' are all close to the supports. The factor is multiplied by the standard load of 10^4 N/m^2 to find the failure load. The result is presented in Figure 18. The averaged failure load is 60.52 kN/m^2 with a standard deviation of 19.07 kN/m^2. The mean value from experiments was 356 kN/m^2, almost a factor 6 larger than the mean simulation result.

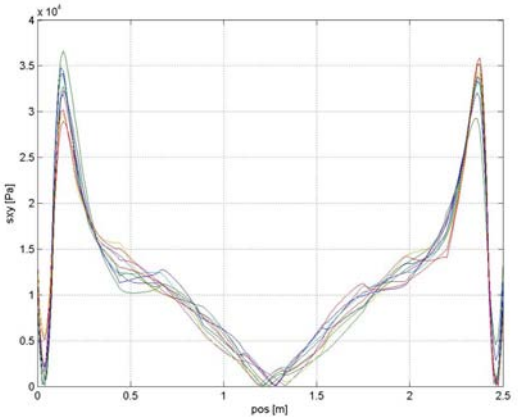

Figure 17. The shear stress profiles for the standard load of 10^4 N/m^2.

5.4. Remarks on COMSOL results

In the test a four-point-loading was used, and in the simulations a uniformly distributed load. The differences in results are limited as indicated by the differences in shear forces along the lintel in Figure 4.

The results of simulation and experiments show some differences due to differences in span length (2.8 m in the test, 2.4m in the simulation).

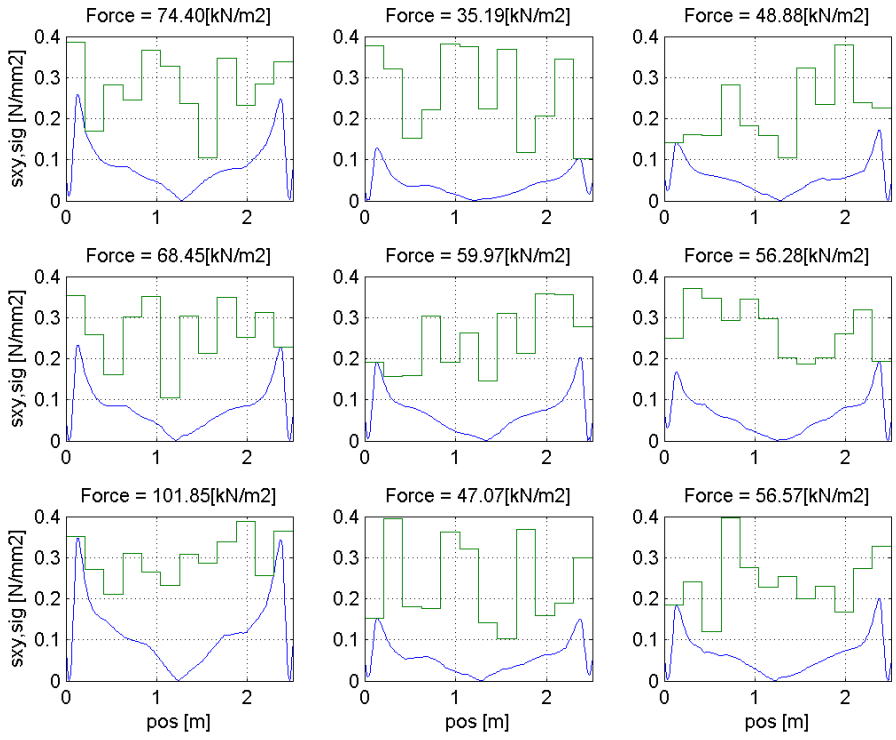

	Fmax kN
1	74.40
2	35.19
3	48.88
4	64.45
5	59.97
6	56.28
7	101.85
8	47.07
9	56.57
avg.	60.52
std.	19.07
CoV	32 %

Figure 18 Shear stress (-) and strength (-) for nine simulated runs

The main difference is due to the assumed shear strength. Mean values for the initial shear strength of 0.33N/mm^2 were found in the test and a value of 0.25N/mm^2 was used in the simulations. In addition, the stresses perpendicular to the shear direction, i.e. perpendicular to the lintel surface would increase the shear strength considerably as shown by equation (1).

In the simulations, the effect of cracking was not taken into account. As observed in the tests, the bed joint between the lintel and masonry will crack at relatively small loads which causes that more load will be transferred via the arch. Consequently, the stress at the foot of the arch and also shear strength will increase.

Both effects mentioned above – larger shear stress due to higher precompression and more load transfer via the arch – could explain the failure load differences between experiments and simulations as follows.
Full loading via the arch, distributed over a contact surface of 0.25 m, results in a pre-stress of 1.25/0.25*360 kN/m^2 = 1800 kN/m^2 and an estimated shear strength according equation (1) of approximately 1.50 N/mm^2. This value is six times the value used in the simulations. When this value would have been used in the simulations the mean failure load would have been 360 N/m^2, almost equal to the mean experimental value.

6. Conclusion and subsequent research

It is concluded that the presented method is promising for simulation of the stochastic behaviour of the experiments. More research is needed to validate the presented methodology.

Further research is required into the effect of stresses perpendicular to the shear direction on the shear strength. The application of a Mohr-Coulomb criterion in the model may be considered.

The shear stress variation is hardly affected by the random variation of the Young's modulus; however, the principal stresses may locally be (much) higher than expected based on a uniform value for the Young's modulus.

A randomly assigned shear strength affects the failure load considerably as shown by Figure 18. Failure may not only be induced by exceeding shear strength. Exceeding the maximum principle tensile stress somewhere in the wall is probably a better criterion. Compressive strength is hardly ever a criterion in masonry.

More detailed subsequent work can concentrate on: the explanation of differences between experimental and simulation results, the effects of energy release when cracking starts, the effect of different support conditions and on the behaviour of the lintel-wall assembly after the first crack occurs.

In all subsequent studies, mentioned above, a considerable number of simulations will be applied (Monte Carlo approach) to study the effects of random material properties.

8. References

Wood, R.H., Studies in composite construction. Part 1: The composite action of brick panel walls supported on reinforced concrete beams, National building studies research paper No 13, HMSO, London, 1952.

NEN EN 1052-3:2006, Methods of test for masonry – part 3: Determination of initial shear strength, European committee for standardization, Brussels, 2001.

Meriam J.L and Kraige L.G., Engineering mechanics, Statics, 6th edition, John Wiley and Sons, Inc., 2008.

Vermeltfoort A.T., Martens D.R.W., Van Zijl G.P.A.G., Brick-mortar interface effects in masonry under compression, Canadian Journal of Civil Engineering, 2007, pp.1475-1485.

Vermeltfoort A.T., Martens D.R.W., Zijl G.P.A.G. van, Laser speckle (ESPI) observation of brick-mortar interface behaviour under compression, Canadian Journal of Civil Engineering, 2007, pp. 1467-1474.